ELSEVIER

Biochemical Pharmacology 62 (2001) 997–1012

Biochemical Pharmacology

Sequestration and phosphorylation of the prostaglandin E_2 EP_4 receptor: dependence on the C-terminal tail

Deborah Slipetz[a,*], Stephanie Buchanan[a], Cameron Mackereth[a], Natalie Brewer[a], Vanessa Pellow[a], Chuan-ming Hao[b], Mohammed Adam[a], Mark Abramovitz[a], Kathleen M. Metters[a]

[a]*Department of Biochemistry and Molecular Biology, Merck Frosst Centre for Therapeutic Research, 16711 Transcanada Hwy., Kirkland, Quebec, Canada, H9H-3L1*

[b]*Department of Medicine, Vanderbilt University Medical School, Nashville, TN 37232, USA*

Received 25 July 2000; accepted 2 February 2001

Abstract

The prostaglandin E_2 (PGE_2) EP_4 subtype is one of four prostanoid receptors that use PGE_2 as the preferred ligand. We have investigated the agonist-mediated regulation of EP_4 using a multifaceted approach. Short-term (30 min) agonist challenge of recombinant EP_4 expressed in human embryonic kidney 293 cells (EP_4-HEK293 cells) with PGE_2 (1 μM) resulted in the desensitization of intracellular cyclic AMP (cAMP) accumulation and a reduction in cell surface [^{3}H]PGE_2 specific binding sites. These events correlated with sequestration of EP_4, as visualized by immunofluorescence confocal microscopy and phosphorylation, as shown by [^{32}P]orthophosphate labeling of the receptor. Stimulation of protein kinase A activity in EP_4-HEK293 cells (10 μM forskolin or 1 mM 8-bromo-cAMP) did not induce EP_4 desensitization, sequestration, or phosphorylation. In contrast, stimulation of protein kinase C activity (100 nM phorbol 12-myristate 13-acetate) attenuated PGE_2-induced adenylyl cyclase activity and increased EP_4 phosphorylation, but did not induce sequestration or a reduction in [^{3}H]PGE_2 specific binding sites. EP_4 receptors containing a third intracellular loop deletion [EP_4 (del. 215–263)] or a carboxyl-terminal tail truncation [EP_4 (del. 355)] of EP_4 were used to demonstrate that the C-terminal tail governs sequestration as well as phosphorylation of the receptor.

Keywords: EP_4; PGE_2; Prostanoid receptor; Desensitization; Sequestration; Phosphorylation; PKA; PKC

1. Introduction

PGE_2 is involved in a number of physiological and pathophysiological events in many tissues throughout the body. The diverse biological effects of PGE_2 are mediated through interaction with specific plasma membrane-bound G-protein-coupled prostanoid EP receptors. The EP receptors can be divided into four subtypes designated EP_1, EP_2, EP_3, and EP_4[1] on the basis of their different pharmacological profiles and signal transduction pathways. In particular, activation of EP_4 leads to accumulation of intracellular cAMP ($[cAMP]_i$) production, through interaction with a cholera toxin-sensitive $G\alpha_s$ [1,2].

The EP_4 receptor has been cloned [3–6], and its function is being defined further. Using EP_4-deficient mice, a crucial role for EP_4 in triggering the closure of the ductus arterious after birth has been elucidated [7]. PGE_2 is a potent modulator of the immune system, and activation of EP_2 and/or EP_4 stimulates isotype switching to IgE and inhibits B-cell activation [8]. Recent evidence also suggests that the potent anabolic effects of PGE_2 in mouse and rat bone marrow are mediated via EP_4 [9,10]. In support of this hypothesis, a

* Corresponding author. Tel.: +1-514-428-3104; fax: +1-514-428-4900.

E-mail address: deborah_slipetz@merck.com (D. Slipetz).

Abbreviations: PGE_2, prostaglandin E_2, GRK, G-protein coupled receptor kinase; PKA, protein kinase A; PKC, protein kinase C; PCR, polymerase chain reaction; DMEM, Dulbecco's modified Eagle's medium; PAS, protein A Sepharose; ECL, electrochemiluminescence; BCA, 2-bicinchoninic acid; IR, immunoreactivity; HBSS, Hanks' buffered salt solution; TBS, Tris-buffered saline; cAMP, cyclic AMP; PMA, phorbol 12-myristate 13 acetate; and β_2-AR, β_2-adrenergic receptor.

[1] Prostanoid receptors are designated following the recommendation of the IUPHAR Commission on Receptor Nomenclature and Classification [1].

0006-2952/01/$ – see front matter
PII: S0006-2952(01)00742-0

potent and selective EP_4 antagonist suppressed PGE_2-mediated increases in trabecular bone volume in young rats [11]. These reports illustrate the emerging importance of EP_4 and the potential for therapeutic intervention with EP_4 agonists in diseases such as osteoporosis.

There are multiple potential intervention points for controlling PGE_2-mediated responses, including ligand production/degradation and/or receptor regulation. Synthesis of PGE_2 occurs via constitutive cyclooxygenase (COX)-1 and/or inducible COX-2 coupled with specific PGE synthases, providing exquisite points of control [12–14]. Subsequently, PGE_2 is cleared from the circulation by a specific PG transporter [15] and is metabolized rapidly to 15-keto-PGE_2 and 13,14-dihydro-15-keto-PGE_2, ligands with diminished biological activity [16]. Little is known, however, about EP receptor regulation in response to agonists. We have chosen to examine the agonist-induced desensitization of the cloned human EP_4 receptor [3], expressed in human embryonic kidney cells (EP_4-HEK293), in order to define the regulation of this receptor.

Desensitization, or the attenuation of agonist-stimulated signaling response despite the continued presence of an agonist, has been studied in detail using the β_2-AR. Receptor phosphorylation by a variety of serine/threonine kinases is one of the most rapid events to occur and is critical in affecting receptor function by ultimately uncoupling the agonist-occupied form of the receptor from the G-protein, thereby limiting receptor function. Phosphorylation of the agonist-occupied receptor by GRKs can occur minutes after agonist stimulation. In addition, the second messenger kinases such as PKA and PKC can phosphorylate the receptor and provide a negative feedback loop from the effector. GRK phosphorylated receptor is a substrate for β-arrestin, which binds to the phosphorylated receptor and promotes uncoupling of G-proteins (for reviews, see Refs. 17–20). With its high-affinity binding to clathrin and its adaptation into clathrin-coated vesicles, β-arrestin has also been implicated in mediating endocytosis of the receptor [21].

In this report, we show that short-term agonist challenge of EP_4 results in attenuation of $[cAMP]_i$ accumulation and sequestration of EP_4, which is accompanied by phosphorylation of the receptor. While activation of PKA does not contribute to EP_4 short-term desensitization, we show that PKC contributes to heterologous EP_4 desensitization. Furthermore, the carboxyl (C)-terminal tail, but not the third intracellular loop of EP_4, contains the determinants responsible for desensitization, sequestration, and phosphorylation of this prostanoid receptor.

2. Materials and methods

2.1. Materials

[^{35}S]Methionine (1175 Ci/mmol), [^{32}P]orthophosphoric acid ($^{32}P_i$) (285.5 Ci/mg), and Enlighten were purchased from NEN Life Science Products. [^{3}H]PGE_2 (187 Ci/mmol) and [^{125}I]cAMP Scintillation Proximity Assay kits, donkey anti-rabbit and sheep anti-mouse Ig horseradish peroxidase linked whole antibodies, and ECL western blotting detection kits were purchased from the Amersham Corp. FLAG-M5 antibody and GSH-agarose were purchased from the Sigma Chemical Co. The Alexa™ secondary antibody conjugates were from Molecular Probes. DMEM, Opti-MEM, penicillin/streptomycin, GENETICIN™ (G418), sodium pyruvate, fetal bovine serum, Enzyme-Free Cell Dissociation Buffer, and LipofectAMINE™ were purchased from Life Technologies Inc. Restriction enzymes were purchased from New England Biolabs. Calf intestinal alkaline phosphatase, protein A Sepharose, and protein G Sepharose were from Pharmacia Biotech. PGE_2, RO-20174, forskolin, and 8-bromo-cAMP were purchased from Biomol. *Taq* DNA polymerase, myokinase, phosphoenol pyruvate, pyruvate kinase, leupeptin, pepstatin, bestatin, and phorbol 12-myristate 13-acetate were from Sigma. ATP, GTP, GTPγS, *N*-glycosidase F, E-64, Pefabloc®, hygromycin B, and *N*-octylglucoside were from Boehringer Mannheim. The BCA protein assay reagent and the Spinzyme PKA kit were from Pierce. pCEP4 and pcDNA3 were from Invitrogen. *Pfu I* DNA polymerase was from Stratagene, and the ABI Prism Dye Terminator Cycle Sequencing Ready Reaction Kit was from Perkin Elmer. Cell-Tak™ and poly-d-lysine-coated 8-well chamber slides and 24-well plates were from Becton-Dickinson.

2.2. Construction of EP_4 deletion mutant receptors

EP_4 from pcDNA1 [3] was subcloned into pcDNA3 with *Eco*RV, and orientation was verified by restriction enzyme analysis. EP_4 (del 215–263) was constructed by PCR amplification using primers 5′-GTCGAGCGCYACCTGGC CATCAAC-3′ (sense) and 5′-TCCCCGCGGCGTGCAT GCGGAGCAGCGC-3′ (antisense) to amplify a fragment corresponding to nucleotides 730-1030 of the EP_4 cDNA [3] that created a novel *Sst*II restriction site at the 3′ end. The primers 5′-TCCCCGCGGGCGCCGAGATCCAGA TG-3′ (sense) and 5′-AAGGAGCGAGAGTGGCCTG AC-3′ (antisense) were used to amplify a fragment corresponding to nucleotides 1179–1530 of the EP_4 cDNA [3] that also created a novel *Sst*II site at the 5′ end. The PCR amplification protocol was performed on a DNA thermal cycler 480 (Perkin Elmer), using *Taq* polymerase and 5 ng of pcDNA3-EP_4 DNA as template, as follows: denaturation at 94° for 60 sec, annealing at 55° for 60 sec, and extension at 72° for 60 sec, for 30 cycles. The resulting 310 and 350 bp fragments were digested with *Pfl*MI and *Sst*II, and *Sst*II and *Ppu*MI, respectively, and isolated following electrophoretic separation in low-melt agarose. These fragments were ligated together at the *Sst*II site and subcloned into pcDNA3-EP_4, which had been digested with *Pfl*MI and *Ppu*MI, creating a deletion in the third intracellular loop of EP_4 of 147 bp, encompassing amino acids 215–263. The ligation of the *Sst*II sites resulted in an insertion of an additional alanine residue giving the following sequence for the third intracellular loop: RMHAAGAIE. The EP_4 (del. 355) mutant was constructed by digesting pcDNA3-EP_4

with *Ppu*MI and *Xba*I (in the polylinker of pcDNA3) to remove the majority of the C-terminal tail after amino acid 355. The large fragment containing pcDNA3-EP_4 was isolated from low-melt agarose, and the 5′ overhangs were filled in with Klenow, followed by ligation to give the truncation mutant at amino acid 355 and an amber stop codon. The sequence of the deletion mutants was verified using the ABI 373 Stretch automated sequencer. Both deletion mutants were subcloned into pCEP4. pcDNA3-EP_4 (del. 215–263) was digested with *Hin*dIII and *Xho*I to release EP_4 (del. 215–263), which was then subcloned into identical sites in pCEP4. pcDNA3-EP_4 (del. 355) was digested with *Hin*dIII and *Bcl*I to release the 1080 bp fragment of EP_4 (del. 355) and 140 bp of pcDNA3 in the SP6 promoter region. This 1220 bp EP_4 (del. 355) fragment was subcloned into the *Hin*dIII and *Bam*HI sites of pCEP4.

2.3. Preparation of human EP_4 antisera

2.3.1. Preparation of EP_4-GST fusion protein

A hydrophilic region in the C-terminal tail of the human EP_4 receptor [3], amino acids (aa) 353–450, was fused to the C-terminus of Sj26, a 26-kDa glutathione S-transferase (GST) encoded by the parasitic helminth *Schistosoma japonicum* [22]. PCR was used to amplify amino acids 353–450 of the EP_4 cDNA [3] with specific 27-mer forward (5′-GGCGGATCCCGCAGGGAGCGCTCCGGA-3′) and reverse (5′-CACCAGGAATTCACTCTCTGAGTCCTG3′) oligonucleotide primers. The forward primer included a BamHI restriction site (underlined) and the reverse primer an EcoRI restriction site (underlined) to allow for directional cloning of the PCR product into pGEX2T. The PCR product and pGEX2T were restricted with BamHI and EcoRI, ligated together and verified by DNA sequencing. The fusion protein was produced in Escherichia coli induced with 0.5 mM isopropyl-β-d-thiogalactopyranoside (IPTG) for 6 hr. The bacteria were lysed by sonication, and the bacterial debris was pelleted by centrifugation (17,200 g) for 10 min at 4°. The GST-EP_4 fusion protein was purified by GSH-agarose chromatography according to the instructions of the manufacturer. After purification, the fusion protein was visualized using SDS–PAGE with a hand-held UV lamp and electro-eluted using an Elutrap Electro–Separation system (Schleicher & Schuell) following the protocol of the manufacturer. The yield was ~1.25 mg of purified fusion protein/500 mL culture. Antiserum production was carried out using the GST-hEP_4 fusion protein in Freund's complete adjuvant in New Zealand White rabbits from HRP Inc. This antiserum was designated MF335.

2.3.2. Preparation of recombinant full-length EP_4 antiserum

Antiserum was raised against full-length recombinant EP_4 and affinity-purified, as described in the international patent application PCT/US99/08214, in the laboratory of Dr. M. Breyer (Vanderbilt University). This antiserum gave an identical profile of EP_4-IR as MF335 by immunoblot analysis. In particular, both MF335 and this EP_4 antiserum gave similar EP_4-IR patterns in the immunofluorescence confocal microscopy studies, although MF335 had a higher background. Therefore, results with the recombinant full-length EP_4 antiserum in the immunofluorescence confocal microscopy are shown.

2.4. FLAG epitope tagging of EP_4 receptor

The FLAG epitope tag (DYKDDDDK) was added to the amino-terminus of EP_4 by PCR amplification using the primers 5′-CCTCAAAGCTTACCATGGACTAC AAAGACGATGACGACAAGGCACCGCCAGCCACT ATCGCGTCCACTCCCG-3′ (sense) and 5′-ACAGGCT GAAGAAGAGCAGAATGAAGG-3′ (antisense), creating a *Hin*dIII site at the 5′ end of the sequence. The PCR amplification protocol was performed on a DNA thermal cycler 480, using *Pfu I* DNA polymerase and 50 ng of pcDNA3-EP_4 DNA as template, as follows: denaturation at 95° for 30 sec, annealing at 60° for 45 sec, and extension at 72° for 30 sec, for 30 cycles. The resulting 345 bp fragment was digested with *Hin*dIII and *Bst*EII to generate a 280 bp fragment that was isolated from low-melt agarose. This fragment was subcloned into pcDNA3-EP_4 that had been digested with *Hin*dIII and *Bst*EII. This construct resulted in EP_4 containing an additional 15 amino acids (MDYKDDDDKAPPATI) at the amino terminus containing the FLAG antigenic sequence followed by a 6 amino acid peptide, with the EP_4 initiating methionine mutated to alanine. The pcDNA3-FLAG (F)EP_4 was verified by DNA sequencing as described above. The FLAG epitope-tagged amino portion of EP_4 was used to replace the corresponding region of pCEP4-EP_4, pCEP4-EP_4 (del. 215–263), and pCEP4-EP_4 (del. 355) by digestion of pcDNA3-FEP_4 with *Hin*dIII and *Sph*I to release a 702 bp FEP_4 that was isolated from low-melt agarose. pCEP4-EP_4, pCEP4-EP_4 (del. 215–263), and pCEP4-EP_4 (del. 355) were also digested with *Hin*dIII and *Sph*I, and the large vector-containing fragments were isolated from low-melt agarose and were ligated to the FEP_4 fragment. All constructs were verified by DNA sequencing.

2.5. Expression of EP_4-containing constructs

Stable clonal expression of EP_4 was achieved by transfection of pCEP4-EP_4, pCEP4-FEP_4 pCEP4-FEP_4 (del. 215–263), and pCEP4-FEP_4 (del. 355) into HEK293 cells stably expressing the Epstein Barr virus nuclear antigen (EBNA) as previously described [23]. Stable bulk expression of pCEP4-EP_4, pCEP4-EP_4 (del. 215–263), and pCEP4-EP_4 (del. 355) was achieved by transfection into human embryonic kidney (HEK293) cells as described above. The transfected cells were maintained in culture for 48 hr, then trypsinized, and grown in the presence of 200 μg/mL of Hygromycin B for 3–4 weeks to select for resistant cells expressing EP_4. Expression of the receptor cDNA

was assessed by receptor binding assays [24]. For all experiments, cells expressing EP_4 (EP_4-HEK293) were used 48–72 hr following typsinization.

2.6. Desensitization of EP_4

Whole cell [^{3}H]PGE_2 binding and cAMP assays were conducted using both suspended and adherent HEK293 cells expressing EP_4 and related constructs. Assays were performed following treatment of the receptor-expressing cells with PGE_2, vehicle, or other reagents as indicated in the figure legends (desensitization protocol). For suspension cell assays, cells were first challenged, then washed three times with PBS, and finally dissociated by incubation in Enzyme-Free Cell Dissociation Buffer. Cells were recovered by centrifugation at 300 *g* for 6 min at 4° and then washed twice with PBS. Cells were finally resuspended in HBSS. All procedures were conducted on ice with ice-cold buffers. Cell viability was $>$ 80% as determined by Trypan Blue exclusion. [^{3}H]PGE_2 binding assays and cAMP accumulation assays were conducted as described below. For adherent cell assays, cells were seeded on 24-well Nunc plates coated with Cell-Tak™ (5 μg/cm^2), were incubated for 48–72 hr, and then were challenged as described above. Following challenge, the cells were placed on ice and washed three times with ice-cold PBS. [^{3}H]PGE_2 binding assays were performed directly on the adherent cells as described below. Adenylyl cyclase assays were performed using membranes prepared from the challenged adherent cells.

2.7. [^{3}H]PGE_2 binding assays

Membrane-based [^{3}H]PGE_2 radioligand binding assays were performed as previously described [23]. Whole cell [^{3}H]PGE_2 binding assays with cells in suspension were performed in a total volume of 0.2 mL with 25 nM PGE_2 (5 nM [^{3}H]PGE_2 supplemented with 20 nM PGE_2) in HBSS. The reaction was started by the addition of 2×10^5 cells per incubation, and non-specific binding was determined in the presence of 10 μM PGE_2. Samples were incubated with shaking for 2 hr at 4°, and separation of the bound and free radioligand was by rapid filtration on GF-C filters as described [23]. [^{3}H]PGE_2 binding assays with adherent cells ($\sim 2 \times 10^5$ cells/well) were performed in a total volume of 0.5 mL with 25 nM PGE_2 (5 nM [^{3}H]PGE_2 supplemented with 20 nM PGE_2) in HBSS. Non-specific binding was determined in the presence of 10 μM PGE_2. The reaction was incubated for 2 hr at 4° and terminated by aspirating the unbound radioligand, followed by one wash with 1 mL HBSS. Cells were solubilized in 0.5 mL of 0.5 N NaOH and counted by liquid scintillation counting.

2.8. cAMP accumulation and adenylyl cyclase assays

Whole cell cAMP accumulation assays were performed with cells in suspension. Incubations were performed in a total of 0.2 mL HBSS containing 100 μM RO-20174 (phosphodiesterase type IV inhibitor). RO-20174 and PGE_2 were added to the incubation mixture in ethanol or DMSO to a final vehicle concentration of 1.1% (v/v) (kept constant in all samples). The reaction was initiated by the addition of 1×10^5 cells per incubation. Samples were incubated at 37° for 10 min, and the reaction was terminated by immersing the samples in boiling water for 3 min. Measurement of cAMP was performed by a [^{125}I]cAMP scintillation proximity assay. Membrane-based adenylyl cyclase assays were performed essentially according to the method of Salomon *et al.* [24] with the following modifications: washed cells were scraped and resuspended in 5 mM Tris–HCl (pH 7.4) with 2 mM EDTA, 0.25 μM soybean trypsin inhibitor, 10 μM leupeptin, and 83 μM benzamidine. The cells were subject to lysis by nitrogen cavitation (600 p.s.i.) for 20 min, and membranes were prepared by differential centrifugation at 4° (1000 *g* for 10 min; 43,000 *g* for 20 min). The membrane pellets were resuspended in 45 mM Tris–HCl (pH 7.5) with 3 mM $MgCl_2$, 1 mM EDTA, 0.25 μM soybean trypsin inhibitor, 10 μM leupeptin, and 83 μM benzamidine. The assay mixture contained 10 μg of membrane protein in 45 mM Tris–Cl (pH 7.5) with 3 mM $MgCl_2$, 1 mM EDTA, 0.12 mM ATP, 0.053 mM GTP, 2.8 mM phosphoenol pyruvate, 0.8 U pyruvate kinase, 1 U myokinase, 100 μM RO-20174, and 0–10 μM PGE_2 in a final volume of 0.1 mL. Samples were incubated for 30 min at 37°, and the reaction was terminated by immersing the samples in boiling water for 5 min. Measurement of cAMP was performed by a [^{125}I]cAMP scintillation proximity assay.

2.9. Immunohistochemistry

The wild-type, mutant, and epitope-tagged EP_4 and control HEK293 cells were seeded on 8-well chamber slides coated with poly-D-lysine and used 2 days later (50% confluence). The cells were then challenged with PGE_2 (1 μM) or vehicle as described in the figure legends and subsequently washed three times with ice-cold PBS. The cells were fixed in 2% (v/v) paraformaldehyde on ice for 30 min followed by two washes in PBS. Non-specific sites were blocked for 30 min with 5% (w/v) fat-free milk in PBS. Cells were then incubated for 1 hr at room temperature with EP_4 antiserum obtained from M. Breyer (Vanderbilt University) (1:500) or FLAG-M5 (10 μg/mL) in 5% (w/v) fat-free milk in PBS, followed by three 2-min washes in PBS. Cells were then incubated for 1 hr at room temperature with Alexa488 donkey anti-goat (EP_4 antiserum) or goat anti-mouse (FLAG-M5 antiserum) IgG conjugate (1:200) in 5% (w/v) fat-free milk in PBS, followed by five 2-min washes in PBS. Slides were mounted using PermaFluor aqueous mountant and scanned using an LSM510 Zeiss confocal scanning microscope.

2.10. Immunoblot analysis

EP_4-HEK293 cells were challenged as described in the figure legends and then washed three times with ice-cold

PBS. Washed cells were frozen in liquid nitrogen, allowed to thaw on ice, and then scraped with 10 mM HEPES (pH 7.4) containing 1 mM EDTA, 4 mM Pefabloc®, 10 μM E-64, 100 μM leupeptin, 73 μM pepstatin, and 10 μM bestatin. Cells were disrupted by three freeze–thaw cycles followed by sonication. Membranes were prepared by differential centrifugation at 4° (1000 *g* for 10 min; 160,000 *g* for 30 min). The final cell pellet was resuspended in 10 mM HEPES (pH 7.4) with 1 mM EDTA and 4 mM Pefabloc®. Membranes (100 μg protein) were solubilized in 2% SDS for 1 hr at room temperature with shaking. Membrane proteins were then deglycosylated in 10 mM $NaPO_4$ (pH 8.0) with 10 mM EDTA, 1% *N*-octylglucoside (w/v), 0.2% SDS (w/v), 4 mM Pefabloc®, and 1 U *N*-glycosidase F for 2 hr at room temperature with shaking. The reaction was terminated by the addition of 3× SDS-sample buffer. Samples (33 μg protein) were separated by SDS–PAGE on 10% Tris-glycine gels and then transferred to 0.45 μm nitrocellulose by electroblotting [25]. Homogeneous transfer was verified on the nitrocellulose with Ponceau S staining. Nonspecific sites on the nitrocellulose were then blocked in 5% fat-free milk (w/v) in TBS [250 mM Tris–HCl (pH 7.5), 1.5 M NaCl] for 30 min. The nitrocellulose blot was incubated with antiserum [MF335 at 1:3000 or FLAG-M5 at 10 μg/mL in 1% fat-free milk (w/v) in TBS] for 2 hr at room temperature and washed in 0.05% Tween-20 (v/v) in TBS for 2 × 20 min and 2 × 5 min. The nitrocellulose blot was incubated with donkey anti-rabbit (MF335) or sheep anti-mouse (FLAG-M5) secondary antibody linked to horseradish peroxidase at 1:2000 in 1% fat-free milk (w/v) in TBS for 1 hr at room temperature and washed as above. Immunoreactivity was revealed by ECL [26].

2.11. Immunoprecipitation analysis

EP_4-HEK293 cells (80% confluence) were labeled with either 100 μCi/mL of [^{35}S]methionine in methionine-free DMEM for 6 hr or 200 μCi/mL of $^{32}P_i$ in phosphate-free DMEM for 2 hr, both at 37°, 6% CO_2. Cells were challenged with PGE_2 or vehicle as described in the figure legends. Membranes were prepared, and proteins were deglycosylated as described for the immunoblot analysis. For immunoprecipitation, deglycosylated membrane proteins (200 μg in 200 μL of 10 mM $NaPO_4$ with 10 mM EDTA, 1% *N*-octylglucoside (w/v), 0.2% SDS (w/v), 4 mM Pefabloc®, and 2 U *N*-glycosidase F) were diluted 5-fold in immunoprecipitation (IP) buffer [10 mM Tris–HCl (pH 7.2) with 300 mM NaCl, 1% Triton X-100]. Immunoprecipitation experiments were conducted using MF335. Samples were pre-cleared using MF335 pre-immune serum pre-bound to 50 μL of PAS for 30 min at 4° on a rotating platform. The pre-cleared samples were incubated with 25 μL MF335 pre-bound to 50 μL of PAS for 90 min at 4° on a rotating platform. The samples were centrifuged at 14,000 *g* for 1 min at 4° to recover immunoprecipitable material and then were washed twice with IP buffer and once with 10 mM Tris–HCl (pH 7.0). Specifically adsorbed proteins were finally eluted from the Sepharose beads by incubation in SDS-sample buffer and were analyzed by SDS–PAGE. Gels containing [^{35}S]methionine-labeled samples were incubated for 10 min in Enlighten and for 10 min in 90% Enlighten/10% glycerol. [^{35}S]methionine- and $^{32}P_i$-labeled proteins were visualized by autoradiography or by phosphoimager analysis (Storm Phosphoimager, Molecular Systems).

2.12. Dephosphorylation

EP_4-HEK293 cells were challenged with PGE_2 (1 μM) or vehicle for 30 min at 37°, 6% CO_2, and membranes were prepared as described for the immunoblot analysis. Membrane proteins (100 μg) were solubilized in 2% (w/v) SDS as described and then dephosphorylated using 0.1 U of alkaline phosphatase in 0.1 mL containing 10 mM Tris-acetate (pH 7.5) with 10 mM Mg^{2+}-acetate, 50 mM K^+-acetate and 0.4% (w/v) SDS for 30 min at 37°. Heat-inactivation of alkaline phosphatase was at 95° for 15 min. Proteins were then deglycosylated by diluting the phosphatase-treated samples 2-fold in 10 mM Tris–HCl (pH 8.0) with 2% (w/v) *N*-octylglucoside, 8 mM Pefabloc® and 0.2% (v/v) β-mercaptoethanol followed by an incubation with 1 U *N*-glycosidase F for 2 hr at room temperature with shaking. The reaction was terminated by the addition of 3× SDS-sample buffer, and samples were analyzed by SDS–PAGE and immunoblot analysis as described.

3. Results

3.1. EP_4 desensitization

We used HEK293 cells expressing recombinant EP_4 (EP_4-HEK293) as the model system for investigating agonist (PGE_2)-induced EP_4 desensitization. Initial saturation analysis of 160,000 *g* membrane fractions from EP_4-HEK293 cells demonstrated that PGE_2 bound with high affinity to a large population of EP_4 receptors in this system [equilibrium dissociation constant (K_D) of 0.6 ± 0.05 nM and a B_{max} of 4.7 ± 0.9 pmol/mg protein, N = 3] [23]. In EP_4-HEK293 cells, activation of EP_4 by PGE_2 caused a concentration-dependent increase in $[cAMP]_i$ production with an EC_{50} of 0.5 ± 0.2 nM, N = 5 (Fig. 1A). Although there is no specific [^{3}H]PGE_2 binding in wild-type HEK293 cells, PGE_2 elicits a small endogenous increase in $[cAMP]_i$ (<10% of EP_4-HEK293 cells) in wild-type HEK293 cells (EC_{50} 300 nM) that we believe is due to an endogenous EP_2 receptor[2] and does not interfere with the interpretation of our results. Desensitization of EP_4 was assessed following agonist treatment of EP_4-HEK293 cells (1 μM PGE_2 for 30 min), which produced a 7-fold rightward shift in the PGE_2

[2] D. Slipetz, unpublished observations.

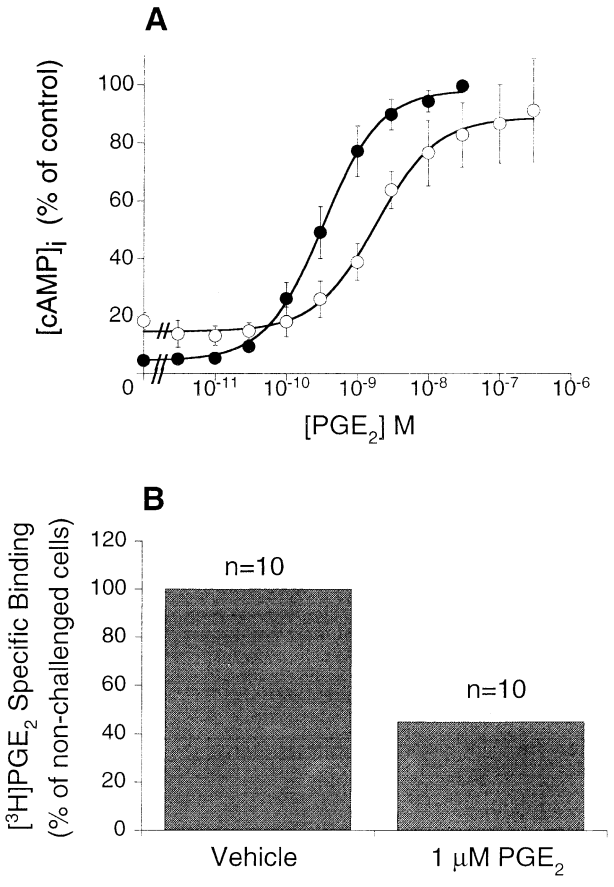

Fig. 1. (A) Whole cell $[cAMP]_i$ accumulation assays in suspended EP_4-HEK293 cells. Cells were treated with vehicle (●, N = 5) or agonist (1 μM PGE_2; ○, N = 4) for 30 min. PGE_2 concentration–response curves (0 to 3×10^7 M) were constructed before and after agonist treatment as described in sections 2.6 and 2.8 of "Materials and methods." Data are expressed as a percentage of the maximal $[cAMP]_i$ produced in the vehicle-treated cells. Values are means ± SEM from experiments performed in duplicate. (B) Whole cell $[^3H]PGE_2$ specific binding assays in suspended EP_4-HEK293 cells. Cells were treated with vehicle or agonist (1 μM PGE_2) for 30 min. Assays were conducted as described in sections 2.6 and 2.7 of "Materials and methods." Data are expressed as a percentage of $[^3H]PGE_2$ specific binding (100% = 5780 ± 590 cpm) detected in vehicle-treated cells. Values are the means ± SEM from N = 10 experiments performed in duplicate.

concentration–response curve (EC_{50} = 3.1 ± 1.3 nM, N = 4) (Fig. 1A).

To measure the total population of EP_4 receptors at the cell surface before and after agonist treatment, the number of detectable $[^3H]PGE_2$ cell surface binding sites was measured using whole cells in suspension under saturating concentrations of radioligand (25 nM $[^3H]PGE_2$) and at 4° (Fig. 1B). After 30 min of agonist treatment, there was a 60% reduction of cell surface $[^3H]PGE_2$ binding sites. Whole cell saturation analysis revealed that this loss of $[^3H]PGE_2$ cell surface binding was due to a decrease in the number of binding sites (B_{max} = 0.73 and 0.4 pmol/mg protein at 0 and 30 min, respectively) and was not caused by changes in the radioligand affinity (K_D = 3.6 and 3.4 nM at 0 and 30 min, respectively). These data demonstrate that agonist challenge of EP_4 expressed in HEK293 cells results in a desensitization of the receptor-mediated adenylyl cyclase response that is accompanied by a reduction in receptor number. These results substantiate the use of this cell line to study EP_4-driven receptor regulation. Throughout this study control wild-type HEK293 cells were employed in parallel experiments and gave negative results. This confirmed the specificity of the EP_4-mediated responses described in this report (data not shown).

3.2. Localization of EP_4 by immunofluorescence

EP_4 localization studies were performed in EP_4-HEK293 cells using confocal immunofluorescent microscopy employing a specific EP_4 antiserum obtained from M. Breyer (Vanderbilt University). Localization studies were performed before and after PGE_2 treatment in order to determine whether the agonist-provoked decreases in cell surface $[^3H]PGE_2$ specific binding sites described above reflect sequestration of EP_4. EP_4-related immunofluorescence was localized predominantly at the plasma membrane in EP_4-HEK293 cells (Fig. 2A). This pattern of immunofluorescence was absent in EP_4-HEK293 cells treated with either pre-immune serum (Fig. 2E), secondary antibody alone (Fig. 2F), or in control wild-type HEK293 cells (Fig. 2G), confirming that the immunofluorescence was EP_4-receptor specific. The limited diffuse staining observed throughout the cytoplasm in EP_4-HEK293 cells was attributable to non-specific interactions as visualization with pre-immune serum alone also showed a light non-specific staining (Fig. 2E). Following a 30-min pretreatment with agonist at 37°, the majority of the specific EP_4-related immunofluorescence disappeared from the plasma membrane and redistributed to intracellular punctate structures typical of early endosomes (Fig. 2B). This agonist-induced EP_4 internalization was inhibited at 4° (Fig. 2, C and D). These data show that internalization of EP_4 is agonist induced and can be monitored quantitatively by measuring $[^3H]PGE_2$ cell surface binding.

3.3. EP_4 phosphorylation

Experiments employing radiolabeling in conjunction with immunoprecipitation were conducted to determine if the EP_4 receptor is phosphorylated in response to agonist challenge. As a first step, a specific EP_4-receptor antiserum (MF335) raised against a GST-fusion protein comprising amino acids 353–450 of the EP_4 C-terminal tail was characterized. EP_4-HEK293 cell membrane proteins (160,000 *g* fraction) were solubilized, deglycosylated, resolved by SDS–PAGE, and visualized by immunodetection using MF335. Specific EP_4-related immunoreactivity (EP_4-IR) migrated with an apparent molecular weight of 50,000 (Fig. 3A, lane 1). The specificity of the signal for EP_4 was confirmed in parallel experiments performed using control wild-type HEK293 cells (data not shown). The antiserum

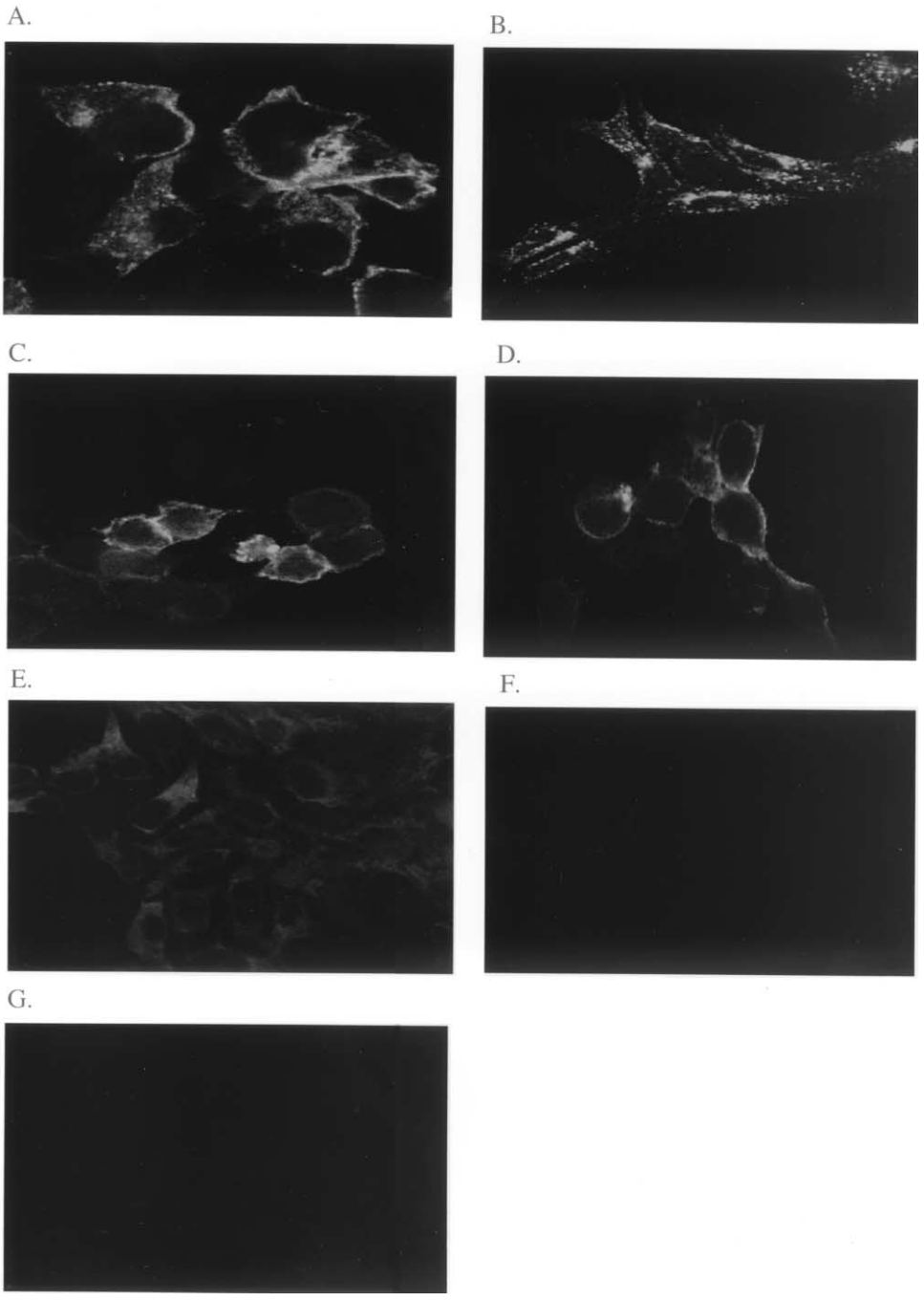

Fig. 2. Localization of EP_4 recombinantly expressed in HEK293 cells by immunofluorescence. EP_4-HEK293 cells were treated with vehicle (A, C, E, F) or agonist (1 μM PGE_2) (B, D) for 30 min at 37° (A, B, E, F) or 4° (C, D). The cells were processed as outlined in section 2.9 of "Materials and methods" using either a specific EP_4 antiserum (A, B, C, D) or pre-immune serum (E), or substituting the primary antibody with blocking buffer (F). Panel G represents control wild-type HEK293 cells treated with vehicle for 30 min at 37°. These images are representative of 5 separate experiments giving comparable results.

was specific for EP_4 and did not cross-react with EP_1, EP_2, $EP_{3\text{-III}}$, DP, FP, IP, and TP receptors recombinantly expressed in HEK293 cells [23] (data not shown). Short-term agonist (0–1 μM PGE_2) treatment (30 min) of EP_4-HEK293 cells resulted in a concentration-dependent decrease in the electrophoretic mobility of EP_4-IR to an apparent molecular weight of 54,000 (Fig. 3A, lanes 1–6). This upward band shift in EP_4-IR was associated with EP_4 activation because it occurred concomitantly with a reduction in cell surface [^{3}H]PGE_2 specific binding sites (Fig. 3B). Both events occurred with an EC_{50} of 1 nM PGE_2, comparable to the K_D for PGE_2 binding to EP_4 in this cell line. In addition, the EP_4-IR upward band shift occurred rapidly. A time-course of agonist challenge (0–30 min)

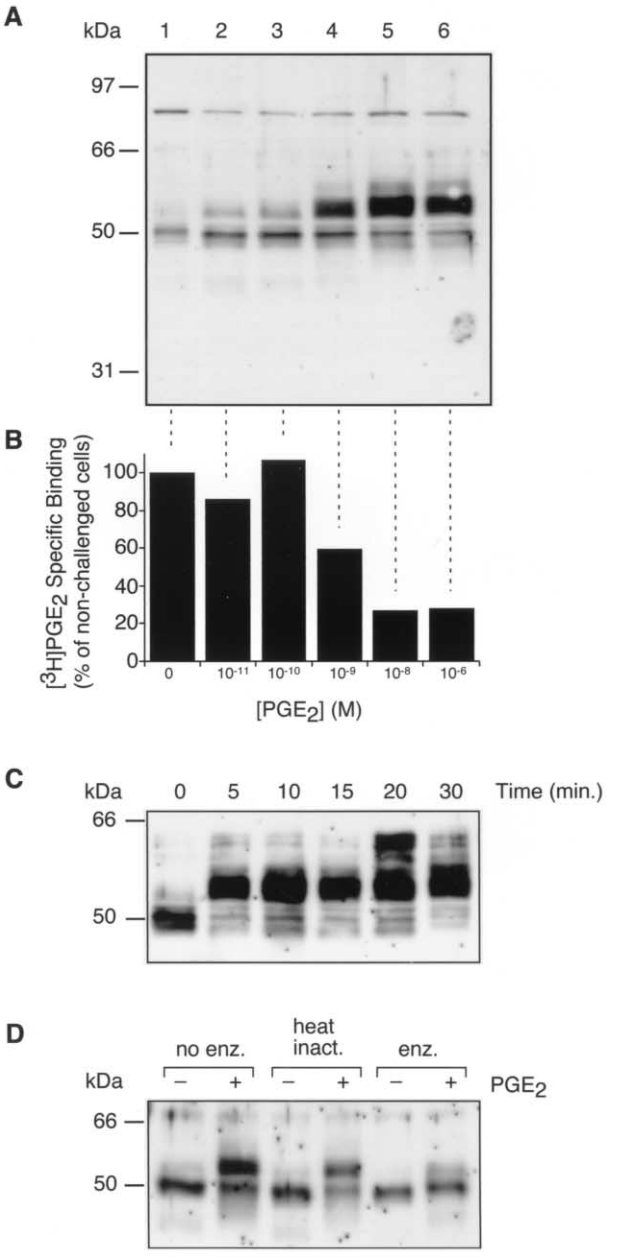

Fig. 3. Immunoblot analysis of EP_4. (A, B) Concentration–response curve of PGE_2-treated EP_4-HEK293 cells. Cells were treated with increasing concentrations (0–10^6 M) of PGE_2 for 30 min and then analyzed by either SDS–PAGE followed by immunoblotting (A) (see section 2.10 of "Materials and methods") or suspended whole cell [^{3}H]PGE_2 specific binding assays (B) (see section 2.7 of "Materials and methods"). Data are expressed as a percentage of [^{3}H]PGE_2 specific binding (100% = 6470 cpm) detected in vehicle-treated cells. These data are representative of 2 experiments giving comparable results. (C) Time-course of PGE_2-treated EP_4-HEK293 cells. Cells were treated for 0–30 min with 1 μM PGE_2 and then analyzed by SDS–PAGE followed by immunoblotting (see section 2.10 of "Materials and methods"). (D) Dephosphorylation of EP_4 following PGE_2 treatment. EP_4-HEK293 cells were pretreated with vehicle or 1 μM PGE_2 for 30 min, and then membrane proteins were subjected to dephosphorylation with alkaline phosphatase (see section 2.12 of "Materials and methods"). Control samples were incubated either without enzyme or with heat-inactivated enzyme as indicated. These data are representative of data from comparable results obtained from 5 independent experiments. Immunoblot analysis was performed with EP_4 MF335 antiserum. Molecular masses (kDa) are shown.

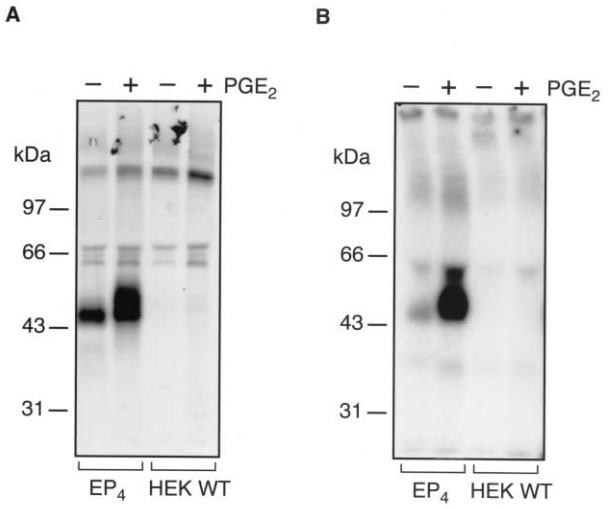

Fig. 4. Immunoprecipitation of EP_4. EP_4-HEK293 or control HEK293 cells were labeled with [^{35}S]methionine (A) or [^{32}P]orthophosphate (B), as described in section 2.11 of "Materials and methods," and challenged for 30 min with vehicle or 1 μM PGE_2 as shown on the top of the corresponding lanes. Radiolabeled immunoreactive material was harvested with the EP_4 MF335 antiserum. Molecular masses (kDa) are shown. These data are representative of comparable results obtained from 3 separate experiments.

illustrated that the majority of EP_4-IR migrated at the higher molecular weight of 54,000 after a 5-min agonist challenge and that there was no further increase in the apparent molecular weight of EP_4-IR over a 30-min period (Fig. 3C).

It was proposed that the EP_4-IR upward band shift was due to agonist-induced receptor phosphorylation. To test this hypothesis, membranes prepared from EP_4-HEK293 cells treated with either vehicle or 1 μM PGE_2 for 30 min were subjected to dephosphorylation by alkaline phosphatase treatment and analyzed by SDS–PAGE and immunodetection (Fig. 3D). As expected, the higher molecular weight EP_4-IR species were detected in the samples treated with PGE_2 but not vehicle. Alkaline phosphatase treatment reversed the majority of the PGE_2-induced upward band shift with EP_4-IR from both vehicle- and agonist-treated cells co-migrating at the original molecular weight of 50,000. The EP_4-IR upward band shift was not reversed by heat-inactivated alkaline phosphatase. These data suggest that most of the EP_4-IR upward band shift is due to phosphorylation. There was residual higher molecular weight EP_4-IR following alkaline phosphatase treatment. The treatment conditions may not have been sufficient to dephosphorylate EP_4 completely or it is possible that the receptor underwent additional post-translational modifications following agonist treatment.

Radiolabeling and immunoprecipitation experiments were performed to confirm that agonist treatment induced phosphorylation of EP_4. Initial studies with metabolic labeling using [^{35}S]methionine demonstrated that the MF335 EP_4 antiserum immunoprecipitated EP_4 from both vehicle- and PGE_2-treated EP_4-HEK293 cells (Fig. 4A). Radiolabeled EP_4-IR from vehicle-treated cells migrated with an

apparent molecular weight of 50,000 in agreement with the results from the immunoblot analysis. In addition, PGE_2 treatment resulted in the appearance of higher molecular weight radiolabeled EP_4-IR, again in agreement with immunoblot analysis. There was no immunoreactivity at this position in HEK293 control cells. Finally, analysis of the [^{35}S]methionine labeled EP_4-IR by densitrometry detected equal amounts of EP_4-related material in the vehicle- and PGE_2-treated samples, indicating that MF335 has the same affinity for all forms of EP_4. EP_4-HEK293 cells were then radiolabeled with [^{32}P]orthophosphate, challenged with either vehicle or PGE_2 for 30 min, and the samples were analyzed by immunoprecipitation with MF335. There was a 15-fold increase in the amount of radioactivity associated with EP_4-IR from the agonist-challenged cells as compared with the vehicle-treated cells (Fig. 4B). There was some endogenous phosphorylation of EP_4 observed in the vehicle-treated samples. The increase in radioactivity associated with agonist treatment of EP_4 in [^{32}P]orthophosphate-labeling studies was calculated by densitometry and was typically 5- to 15-fold. These results confirm that agonist challenge with PGE_2 results in phosphorylation of EP_4. Taken together these data also demonstrated that agonist-induced phosphorylation of EP_4 results in an increase in the apparent molecular weight of EP_4, as assessed by SDS–PAGE followed by immunoblot analysis. This upward band shift was used in future experiments, described below, as an index of EP_4 phosphorylation.

3.4. Second messenger kinase activation

The following experiments were designed to determine if either PKA or PKC plays a role in EP_4 desensitization/phosphorylation. PKA is a second messenger kinase activated by $[cAMP]_i$. Known activators of PKA include forskolin, which binds adenylyl cyclase, and 8-bromo-cAMP, which stimulates PKA directly. Because agonist activation of EP_4 increases $[cAMP]_i$, receptor-mediated activation of PKA was examined in EP_4-HEK293 cells. Cytosolic PKA activity increased 40-fold after challenge of EP_4-HEK293 cells with 1 μM PGE_2, 10 μM forskolin, or 1 mM 8-bromo-cAMP, as compared with the basal level seen with vehicle alone, demonstrating that agonist activation of EP_4 in turn activates PKA (Fig. 5A). In addition, there are two consensus PKA phosphorylation sites in the third intracellular loop (i3) of EP_4 (Fig. 6). Therefore, the role of PKA in mediating EP_4 desensitization, sequestration, and phosphorylation was examined. There are also four consensus PKC phosphorylation sites in the C-terminal tail of EP_4 and one in the third intracellular loop (i3) (Fig. 6). Therefore, the tumor promoter PMA, a well-known activator of PKC, was utilized to examine whether PKC mediated heterologous EP_4 desensitization. At this stage, a membrane adenylyl cyclase assay and an adherent whole cell [^{3}H]PGE_2 binding assay were developed to facilitate the experiments and were employed in these and future experiments.

Adenylyl cyclase assays were employed to measure EP_4 functional desensitization. PGE_2 provoked a concentration-dependent increase in EP_4-mediated adenylyl cyclase activity with an EC_{50} of 0.54 $\pm$ 0.14 nM (Fig. 5B). Challenge of EP_4-HEK293 cells with 1 μM PGE_2 caused a 10-fold rightward shift (EC_{50} = 5.5 $\pm$ 1.2 nM) in the PGE_2 concentration–response curve. These values are in excellent agreement with the data obtained using whole cell $[cAMP]_i$ accumulation assays. In the membrane-based assay, however, agonist treatment also resulted in a significant decrease in both the basal ($P < 0.001$) and maximal ($P < 0.02$) adenylyl cyclase activities (Fig. 5B). This is probably due to a reduction in the EP_4 constitutive activity that appears in the membrane-based assay. We have systematically varied the EP_4 density in HEK293 cells and have shown that increased receptor expression increases the basal functional activity of EP_4 (M. Abramovitz, unpublished results). The EP_4 constitutive activity is, therefore, probably related to the relatively high level of expression of EP_4 in these cell lines. Treatment of EP_4-HEK293 cells with 10 μM forskolin did not desensitize the PGE_2-mediated adenylyl cyclase response, with an EC_{50} = 0.53 $\pm$ 0.12 nM and basal and maximal activities that were indistinguishable from vehicle-treated cells. In contrast, when EP_4-HEK293 cells were challenged with 100 nM PMA, a 5-fold rightward shift in the concentration–response curve was obtained (EC_{50} = 2.5 $\pm$ 0.2 nM), and although the maximal activity did not differ significantly from that of the vehicle-treated cells ($P = 0.97$), the basal activity was significantly lower ($P < 0.001$).

Measurement of whole cell specific binding using the adherent cell assay protocol indicated that a 30-min treatment with 1 μM PGE_2 provoked a 70 $\pm$ 2% decrease in cell-surface [^{3}H]PGE_2 specific binding sites (Fig. 5C). This is in excellent agreement with the suspension cell assay protocol utilized in Fig. 1B. Challenge of EP_4-HEK293 cells with 1 mM 8-bromo-cAMP did not provoke any losses in cell-surface binding sites (105 $\pm$ 3%). In contrast, 100nM PMA treatment significantly ($P < 0.02$) increased the number of cell-surface [^{3}H]PGE_2 specific binding sites to 117 $\pm$ 5% of control values. Combining 1 μM PGE_2 with either 1 mM 8-bromo-cAMP or 100 nM PMA resulted in a reduction in cell-surface [^{3}H]PGE_2 specific binding sites similar to that produced by PGE_2 challenge alone [67% (avg. N = 2) and 69 $\pm$ 7%, respectively] (Fig. 5C).

The results from the whole cell binding analysis suggested that activation of the second messenger kinases PKA and PKC would not induce EP_4 sequestration. This was confirmed by confocal immunofluorescence microscopy. EP_4-related immunofluorescence remained localized to the plasma membrane in EP_4-HEK293 cells treated with either 1 mM 8-bromo-cAMP or 100 nM PMA. This reveals that activation of PKA or PKC does not induce EP_4 sequestration (Fig. 5, D and F). EP_4 sequestration was induced, however, when EP_4-HEK293 cells were challenged with 1 μM PGE_2 in combination with either 1 mM 8-bromo-cAMP or 100 nM PMA (Fig. 5, E and G). In these examples, punctate staining of EP_4-related immunofluorescence in the

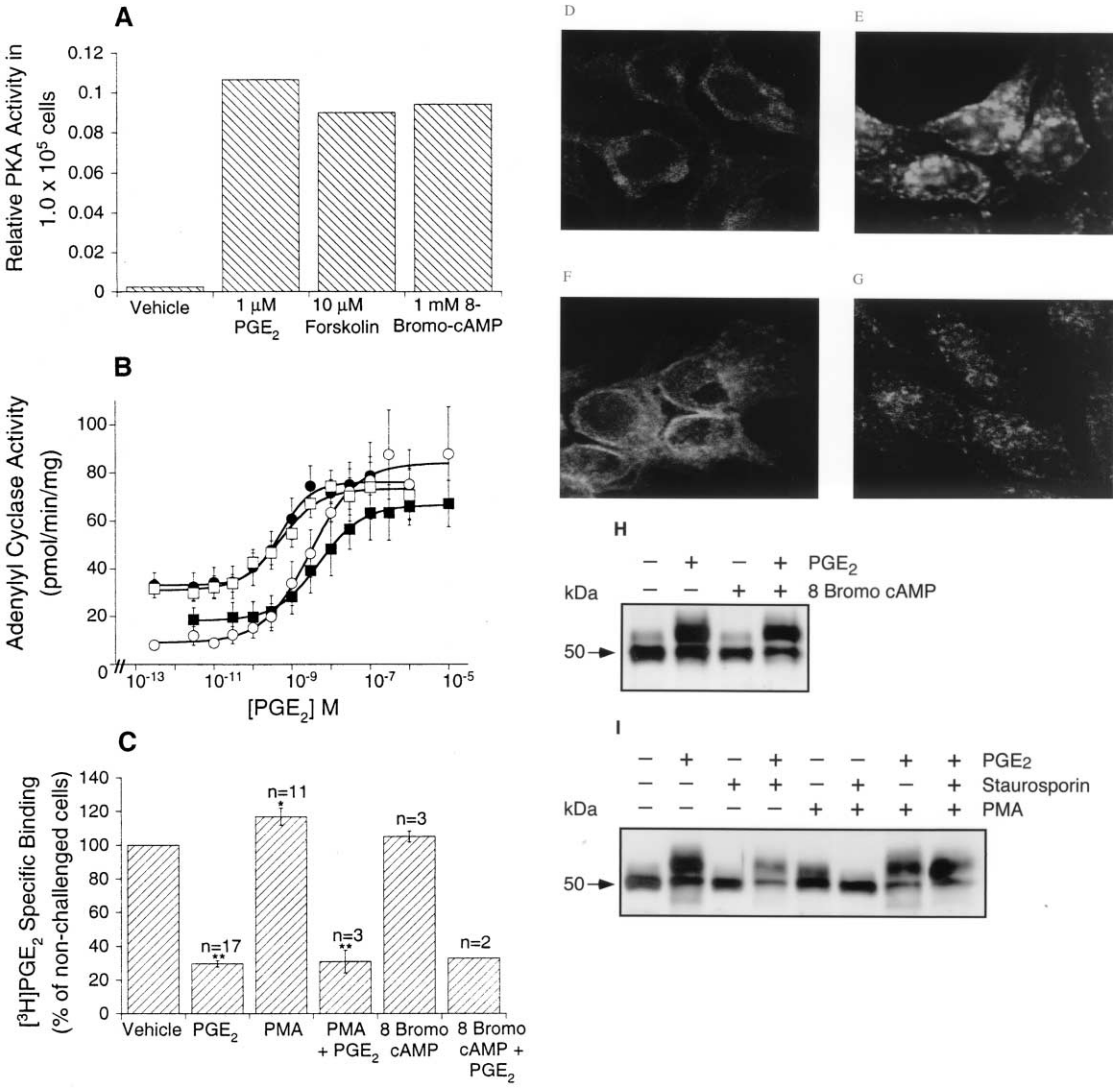

Fig. 5. Regulation of EP_4 by PKA and PKC. (A) Activation of PKA in EP_4-HEK293 cells challenged for 30 min with 1 μM PGE_2, 10 μM forskolin, or 1 mM 8-bromo-cAMP. PKA activity was measured in whole cell lysates using a Spinzyme PKA kit. These data are representative of data from 2 experiments performed in triplicate. (B) Adenylyl cyclase assays in EP_4-HEK293 cells challenged for 30 min with vehicle (●), 1 μM PGE_2 (■), 10 μM forskolin (❐), or 100 nM PMA (❍), as described in sections 2.6 and 2.8 of "Materials and methods." Data are expressed as means ± SEM from 3 experiments performed in duplicate. (C) Whole cell [^{3}H]PGE_2 specific binding assays using adherent EP_4-HEK293 cells were performed as described in sections 2.6 and 2.7 of "Materials and methods." Cells were challenged for 30 min with the indicated reagents. Data are expressed as a percentage of [^{3}H]PGE_2 specific binding in the vehicle-treated cells (100% = 10,180 ± 950 cpm). Values are the means ± SEM from the indicated number of experiments performed in triplicate. The 8-bromo-cAMP + PGE_2 value represents the mean of 2 experiments with the individual values equal to 42 and 24%. The (**) and (*) indicates significance at $P < 0.001$ and $P < 0.05$, respectively, compared with vehicle-treated samples. (D–G) Immunofluorescence localization of EP_4. EP_4-HEK293 cells were treated with 1 mM 8-bromo-cAMP (D), 1 μM PGE_2 + 1 mM 8-bromo-cAMP (E), 100 nM PMA (F), or 1 μM PGE_2 + 100 nM PMA (G) for 30 min at 37°, as described in section 2.9 of "Materials and methods" using the EP_4 specific antiserum (Vanderbilt University). These data are representative of data from 3 experiments performed in duplicate. (H, I) SDS–PAGE and immunoblot analysis of EP_4-HEK293 cells pretreated for 30 min with the reagents shown. Immunoblot analysis was performed as described in section 2.10 of "Materials and methods" using EP_4 MF335 antiserum. Only the region of the immunoblot encompassing the EP_4-IR is shown (48–61 kDa). These data are representative of data from 1 of 3 comparable experiments.

cytoplasm had a similar distribution pattern to that obtained by challenge with PGE_2 alone. This confirms that agonist activation of EP_4 drives sequestration independently of PKA and PKC activation.

Finally, the effect of PKA or PKC activation on EP_4 phosphorylation was studied using the EP_4-IR band shift as a surrogate marker. Immunoblot analysis of EP_4-HEK293 cells revealed that there was no increase in the apparent molecular weight of EP_4-IR from cells treated with 1 mM 8-bromo-cAMP alone, as compared with the increase routinely observed with PGE_2 treatment (Fig. 5H). Treatment of EP_4-HEK293 cells with both 1 μM PGE_2 and 1 mM 8-bromo-cAMP resulted in a profile identical to that observed with PGE_2 alone. These results show that agonist, but not PKA, activation is responsible for the majority of EP_4 phosphorylation (Fig. 5H). In contrast, treatment with

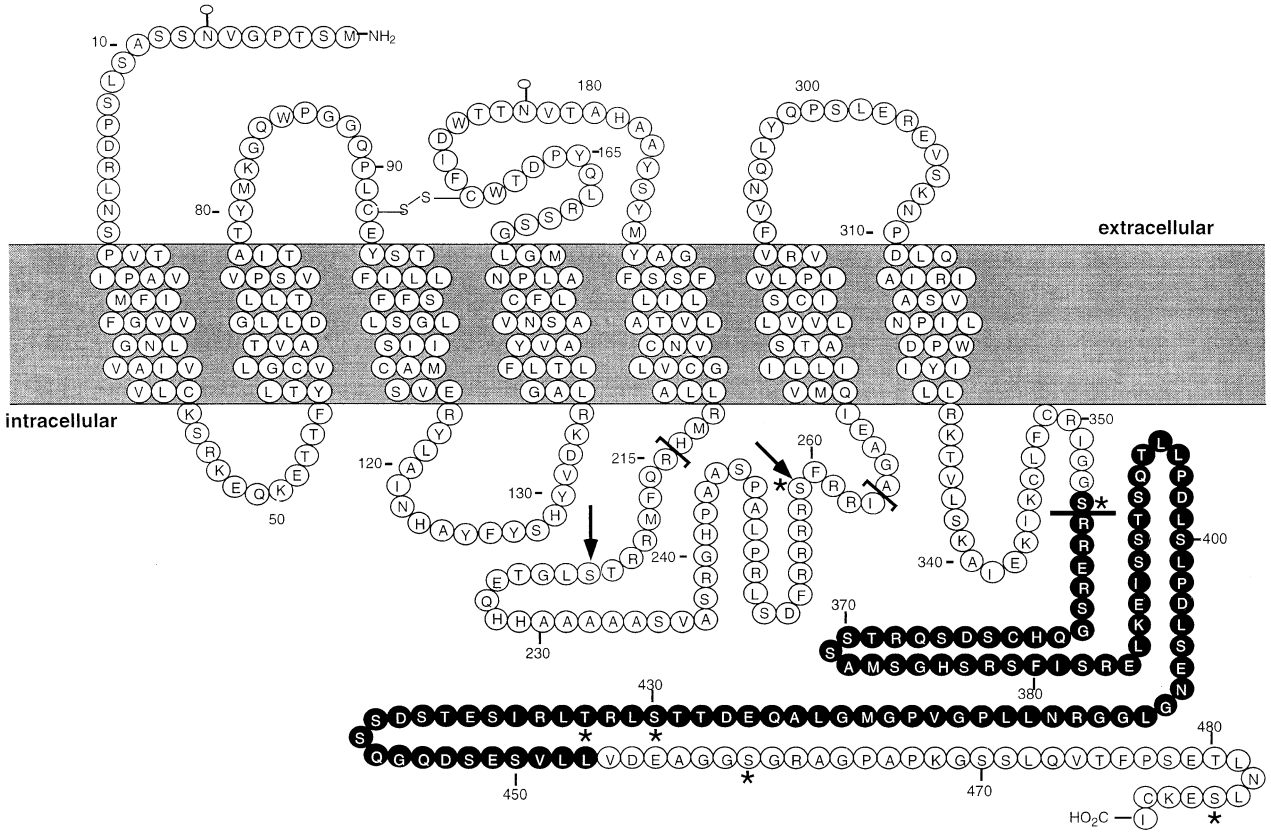

Fig. 6. Schematic representation of the amino-acid sequence of EP_4. Arrows indicate PKA consensus phosphorylation sites. Asterisks indicate PKC consensus phosphorylation sites. Single bar brackets encompass the third intracellular loop deletion. A solid line represents the C-terminal tail deletion. Solid circles indicate the region utilized for the GST-fusion protein in the generation of the MF335 antiserum.

100 nM PMA induced the appearance of a higher molecular weight form of EP_4-IR migrating at 53 kDa, that was clearly and consistently distinct from the agonist-mediated form migrating at 54 kDa (Fig. 5I). The appearance of the PMA-induced EP_4-IR 53-kDa species, but not the agonist-induced EP_4-IR 54-kDa species, was inhibited significantly by pretreating EP_4-HEK293 cells for 15 min with 1 μM staurosporin, a PKC inhibitor. Furthermore, treatment with 100 nM PMA in combination with 1 μM PGE_2 provoked an EP_4-IR band shift to 54 kDa that was insensitive to staurosporin inhibition, suggesting that agonist-induced EP_4 phosphorylation is the predominant pathway. Taken together, these data show that PKA activation does not play a role in EP_4 desensitization and that PKC may have a minor role in the desensitization of only the adenylyl cyclase response.

3.5. EP_4 deletion mutants

To identify the regions of EP_4 containing the determinants of receptor desensitization and phosphorylation, two deletion mutants were constructed. EP_4 (del. 215–263) had 48 amino acids of i3 deleted, which removed the two PKA and one of five PKC consensus phosphorylation sites. EP_4 (del. 355) was a truncation of 133 amino acids from the C-terminal tail, which removed 34 serine and threonine residues including four of the five PKC consensus sites. New bulk stable cell lines were constructed for EP_4, EP_4 (del. 215–263), and EP_4 (del. 355) in HEK293 cells. Membrane saturation analysis with [^{3}H]PGE_2 showed that the new bulk EP_4 stable cell line had a similar K_D (1.1 nM) but a lower B_{max} (2.6 pmol/mg protein) than the clonal stable EP_4-HEK293 cell line used in the studies described above. In comparison, the deletion mutants EP_4 (del. 215–263) and EP_4 (del. 355) had K_D values of 10 and 1 nM, respectively, and B_{max} values of 1 and 3.6 pmol/mg protein, respectively. Adenylyl cyclase assays confirm that these deletion mutants were functionally coupled to their effector system. Overall, the EP_4-driven adenylyl cyclase response was less sensitive (7-fold) in the bulk EP_4-HEK293 cells compared with the clonal EP_4-HEK293 cells, which is probably a reflection of the lower receptor number detected in the bulk cell line. These data substantiate the use of these mutants and cell lines for studying EP_4 desensitization.

Adenylyl cyclase assays were performed to assess the functional desensitization of the EP_4 mutants following a 30-min treatment with 1 μM PGE_2. Wild-type EP_4 displayed the expected rightward shift (18-fold) in the PGE_2 concentration–response curves following agonist treatment,

with EC_{50} values increasing from 3.6 ± 0.7 to 66 ± 18 nM (Fig. 7A). Similarly, the PGE_2-mediated adenylyl cyclase response for EP_4 (del. 215–263) showed desensitization, with EC_{50} values increasing 5-fold from 21 ± 6.0 to 108 ± 16 nM. In contrast, desensitization of EP_4 (del. 355) was not observed, as sensitivity to PGE_2 was unaffected by the agonist treatment (EC_{50} = 7.8 ± 1.9 and 6.2 ± 1.7 nM, for vehicle- and PGE_2-treated cells, respectively) (Fig. 7, B and C).

Whole cell [^{3}H]PGE_2 specific binding was also monitored following a 30-min treatment with 1 μM PGE_2 (Fig. 7D). Again, as expected, agonist treatment of wild-type EP_4 resulted in a reduction (73 ± 3%) in cell-surface [^{3}H]PGE_2 specific binding sites. EP_4 (del. 215–263) displayed similar sensitivity to the agonist as the wild-type EP_4 with an 83 ± 3% loss of cell-surface [^{3}H]PGE_2 binding sites. In contrast, the truncation of the C-terminal tail dramatically attenuated this loss of cell-surface [^{3}H]PGE_2 specific binding sites, as only a 23 ± 0.4% reduction was observed.

Because the truncation of the EP_4 C-terminal tail removed the sequence encoding the epitopes of both EP_4 antisera, we were unable to assess the sequestration by confocal immunofluorescence microscopy or the phosphorylation state of EP_4 (del. 355). Therefore, the FLAG epitope sequence "DYKDDDDK" was inserted at the N-terminus of EP_4, EP_4 (del. 215–263), and EP_4 (del. 355). The insertion of the FLAG epitope did not result in differences in the behavior of the receptors as measured by saturation analysis [K_D = 3, 6, and 1 nM for FEP_4, FEP_4 (del. 215–263), and FEP_4 (del. 355), respectively], adenylyl cyclase activities [EC_{50} 3.3, 22, and 12 nM for FEP_4, FEP_4 (del. 215–263), and FEP_4 (del. 355), respectively], and the desensitization profile following agonist treatment as measured by the rightward shift of the PGE_2 concentration–response curve [10- and 3-fold shift for FEP_4 and FEP_4 (del. 215–263), respectively, and no shift for FEP_4 (del. 355)] (data not shown).

The phosphorylation state of FEP_4, FEP_4 (del. 215–263), and FEP_4 (del. 355) following agonist treatment was again investigated by SDS–PAGE and immunodetection using the upward band shift as a surrogate marker (Fig. 7E). Immunoblot analysis indicated that FEP_4-IR migrated as a doublet at 54 and 57 kDa. The addition of the FLAG epitope, therefore, increased the EP_4-IR apparent molecular weight by 4000. A 30-min treatment with 1 μM PGE_2 induced phosphorylation of FEP_4 as visualized by an increase in FEP_4-IR from 57 to 61 kDa. Similarily, FEP_4 (del. 215–263)-IR migrated as a doublet at 46 and 51 kDa. The 51 kDa band represented the phosphorylated form of FEP_4 (del. 215–263)-IR as the intensity of this band was increased 5-fold after agonist treatment. In contrast, the migration of FEP_4 (del. 355)-IR at 40 kDa was unaffected by PGE_2 treatment, indicating that this receptor mutant is not phosphorylated upon agonist challenge. These data strongly indicate that the major sites of agonist-mediated phosphorylation lie in the C-terminal tail of the EP_4 receptor and not in the i3 loop.

Immunofluorescence microscopy using FLAG-M5 antiserum was employed to determine whether the agonist-induced sequestration of FEP_4 (del. 215–263) and FEP_4 (del. 355) was affected by their respective i3 and C-terminal deletions (Fig. 8). EP_4 was localized to the plasma membrane in the FEP_4, the FEP_4 (del. 215–263), and the FEP_4 (del. 355) HEK293 cell lines as shown by the distribution of FLAG-related immunofluorescence (Fig. 8, A, C, and E). Thus, neither the epitope tagging of EP_4 nor the i3 or C-terminal tail deletions affected its subcellular localization. Visualization of FLAG-related immunofluorescence after agonist treatment revealed that both FEP_4 and FEP_4 (del. 215–263) sequestered into intracellular punctate compartments, but FEP_4 (del. 355) remained localized at the plasma membrane (Fig. 8, B, D, and F) These data show that the determinants for EP_4 sequestration are also located in the C-terminal tail of EP_4.

4. Discussion

The data presented in this study have developed an extensive desensitization paradigm for EP_4 recombinantly expressed in one cell system. This elucidation of the mechanisms of EP_4 desensitization show that agonist treatment induces desensitization of functional activity, losses in cell surface binding sites, sequestration, and EP_4 phosphorylation. Studies with EP_4 deletion mutants support the hypothesis that the C-terminal tail contained the determinants that controlled these processes.

Desensitization of EP_4 functional response was monitored by both whole-cell $[cAMP]_i$ accumulation and membrane adenylyl cyclase assays. Both methods indicated that EP_4 was desensitized by agonist treatment as shown primarily by rightward shifts in the PGE_2 concentration–response curves. The specific binding of [^{3}H]PGE_2 to whole cells gave a quantitative reflection of agonist-induced EP_4 sequestration into the cell because saturation analysis indicated that the cell-surface receptor number decreased, but the affinity for the residual receptors did not change. To provide additional evidence for EP_4 sequestration, we utilized immunofluoresence confocal microscopy. Agonist activation of many receptors promotes endocytosis and internalization by either clathrin-coated or non-coated vesicle pathways (for a review, see Ref. 19). In agreement, EP_4 receptor sequestration was observed post agonist challenge with the redistribution of the majority of EP_4 immunoreactivity into intracellular aggregates that probably represent endosomes. Our data greatly expand upon a previous study reporting desensitization of the EP_4 adenylyl cyclase response in EP_4 CHO cells [16].

A hallmark of G-protein-coupled receptor (GPCR) desensitization is the rapid phosphorylation of the receptor that appears within minutes of agonist stimulation [18]. In this report, we show that EP_4 is also rapidly phosphorylated within 5 min of agonist challenge. Direct phosphorylation of EP_4 was confirmed by immunoprecipitation of the receptor using our specific EP_4 MF335 antiserum from EP_4-HEK293 cells la-

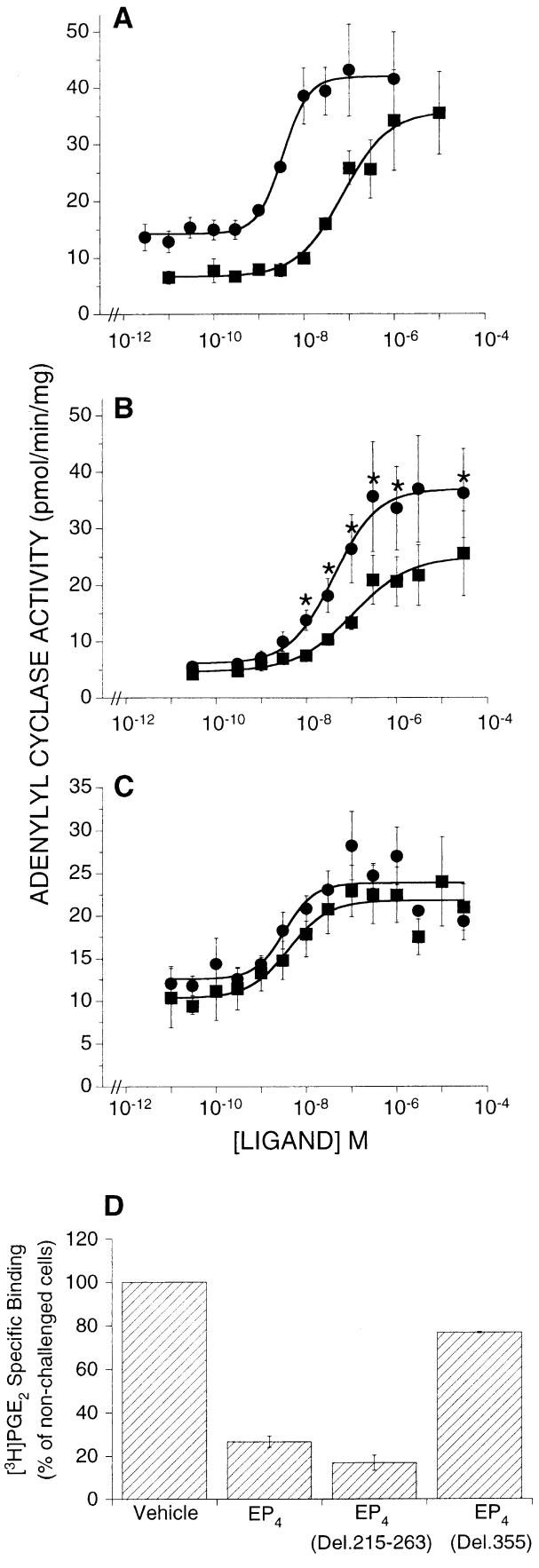

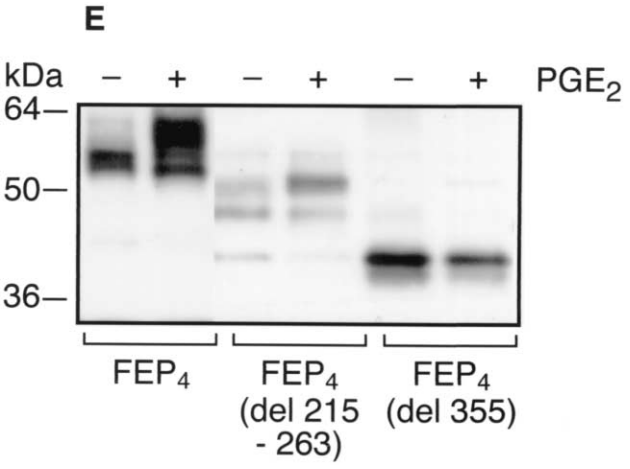

beled with $^{32}P_i$. Agonist-induced phosphorylation of EP_4 reduced the electrophoretic mobility of the receptor, and this was visualized by immunoblotting as an increase in the apparent molecular weight of EP_4-IR. This upward "band shift" was used as an index of receptor phosphorylation throughout this study. The use of this marker was validated by experiments showing that dephosphorylation of EP_4 by alkaline phosphatase treatment could reverse the band shift.

EP_4 phosphorylation and sequestration were directly linked as both occurred concomitantly over an identical agonist concentration range with comparable EC_{50} values (~1 nM) and maximal responses (10 nM). These data associating EP_4 phosphorylation and sequestration support the hypothesis that β-arrestin binding to agonist-activated, phosphorylated EP_4 may mediate its internalization via clathrin-coated pits, as occurs with other GPCRs. Future experiments using β-arrestin fluorescent conjugates and confocal microscopy will define further its role in EP_4 sequestration.

Both the GRKs and the second messenger kinases are principal regulators of GPCR phosphorylation and uncoupling [17,27,28]. To understand further the kinases respon-

Fig. 7. (Opposite) Deletion mutant analysis. Adenylyl cyclase assays in bulk stable EP_4-HEK293 (A), EP_4 (del. 215–263) (B), and EP_4 (del. 355) (C) cells challenged for 30 min with vehicle (●) or 1 μM PGE_2 (■), as described in sections 2.6 and 2.8 of "Materials and methods." The (*) represents significance at $P < 0.05$. Data are expressed as means ± SEM from 5 experiments performed in duplicate. (D) Whole cell [^{3}H]PGE_2 specific binding assays using bulk stable adherent EP_4-HEK293, EP_4 (del. 215–263) and EP_4 (del. 355) cells, as described in sections 2.6 and 2.7 of "Materials and methods." Cells were challenged for 30 min with vehicle or 1 μM PGE_2. Data are expressed as a percentage of [^{3}H]PGE_2 specific binding in the vehicle-treated cells that was taken as 100% for each construct (100% in EP_4 = 5230 ± 920 cpm, EP_4 (del. 215–263) = 3650 ± 900 cpm, and EP_4 (del. 355) = 16,140 ± 3680 cpm). Values are the means ± SEM from 3 experiments performed in triplicate. (E) SDS–PAGE and immunoblot analysis of FEP_4-HEK293, FEP_4 (del. 215–263), and FEP_4 (del. 355) cells pretreated for 30 min with 1 μM PGE_2. Immunoblot analysis was performed as described in section 2.10 of "Materials and methods" using FLAG-M5 antiserum as described. Only the region of the immunoblot encompassing the EP_4-IR is shown (36–64 kDa). These data are representative of data from 3 comparable experiments.

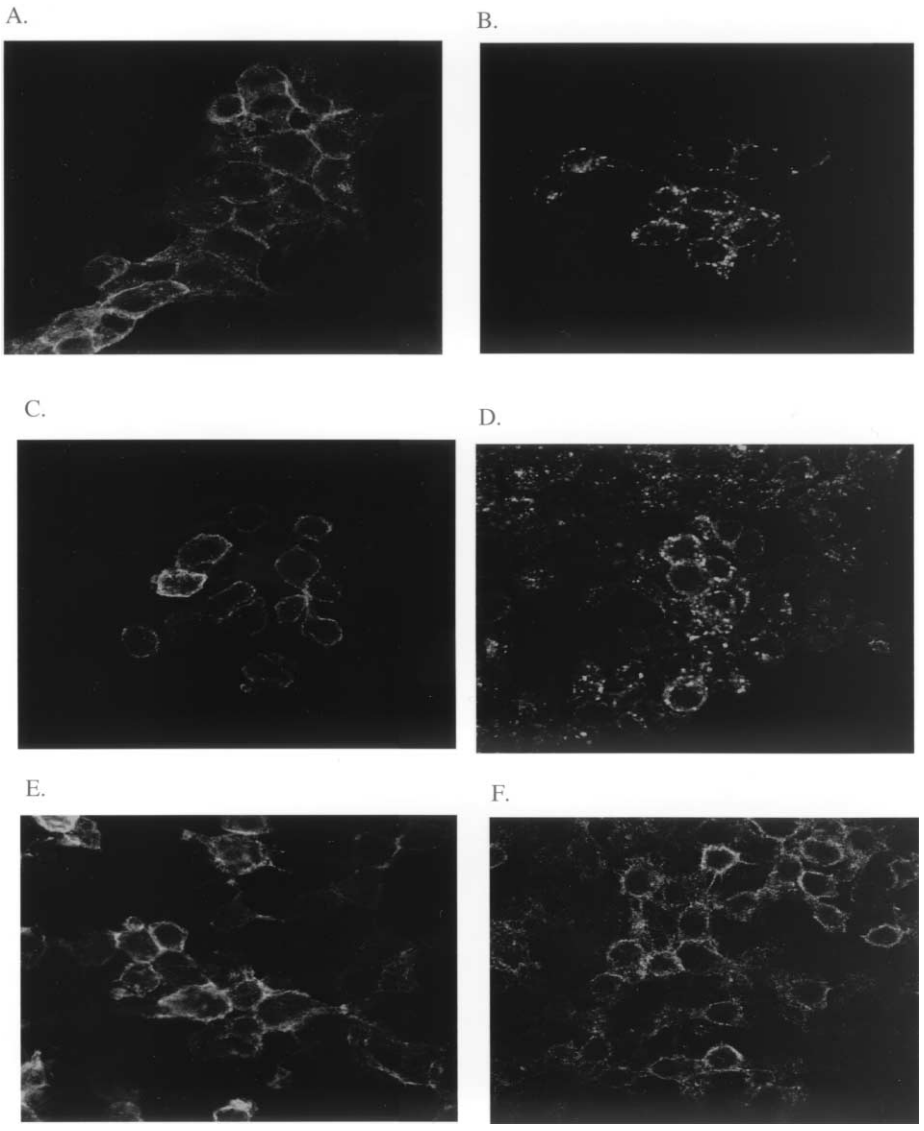

Fig. 8. Immunofluorescence localization of FEP_4 (A, B), FEP_4 (del. 215–263) (C, D), and FEP_4 (del. 355) (E, F) in HEK293 cells. Cells were treated with vehicle (A, C, E) or 1 μM PGE_2 (B, D, F) for 30 min at 37°, as described in section 2.9 of "Materials and methods" using FLAG-M5 antiserum. These data are representative of data from 3 comparable experiments performed in duplicate.

sible for EP_4 phosphorylation, we investigated the roles of PKA and PKC. Both forskolin and 8-bromo-cAMP activated PKA in EP_4-HEK293 cells, but they did not provoke desensitization, sequestration, or increased phosphorylation of EP_4. Agonist activation of EP_4 is not known to stimulate PKC. However, there are five PKC consensus phosphorylation sequences in EP_4, and the potential for heterologous desensitization by activators of PKC was examined. Challenge of EP_4-HEK293 cells with PMA caused a desensitization of the EP_4 adenylyl cyclase response and a slight, but significant, increase in EP_4 binding sites. Immunofluorescence microscopy confirmed that PMA did not induce EP_4 sequestration. This separation of PMA-induced desensitization from sequestration indicates a divergence of these two pathways. In fact, receptor endocytosis is thought to be mediated by β-arrestin binding of a GRK-phosphorylated agonist occupied receptor [29,30]. For the β_2-AR, endocytosis is mediated via direct interaction of β-arrestin and clathrin [20] via recruitment of the clathrin adaptor AP-2 [31]. If this is the case for EP_4, then PKC phosphorylation would not be expected to promote sequestration. Instead, the role of PKC could be to cause a functional desensitization of EP_4 by uncoupling G-proteins through receptor phosphorylation. In support of this hypothesis, PMA caused EP_4 phosphorylation, although this was not as pronounced as that induced by the agonist. The PMA-induced EP_4 phosphorylation was mechanism-based as it was reversed by the PKC inhibitor staurosporin. Preincubation of the cells with both PMA and PGE_2 resulted in an EP_4 phosphorylation pattern comparable to that found with agonist alone. This suggests that agonist-induced EP_4 phosphorylation is the predominant mechanism. Because PMA in-

creased the number of cell-surface EP_4 receptors, it is possible that the increase in EP_4 phosphorylation observed with PMA merely reflects an increase in the basal level of EP_4 phosphorylation. However, our findings are supported by a previous report describing PMA-induced phosphorylation of EP_4 in COS-7 cells, although this study did not monitor any other aspects of EP_4 desensitization [32]. In conclusion, PMA-induced desensitization of the adenylyl cyclase response suggests that EP_4 may be desensitized heterologously when cellular activation of PKC occurs and that this event may occur through EP_4 phosphorylation.

The lack of direct effects on agonist-mediated receptor phosphorylation by activation of PKA or PKC suggests a strong role for the GRKs in this process. Indeed, the C-terminal tail of EP_4 contains 38 serine and threonine residues as well as multiple acidic amino-acid pairs that have been strongly linked as recognition sequences for the GRKs [33–37]. The HEK293 cells have been shown to contain GRK2 and GRK5 [38], and our own studies show the presence of GRK2, -4, and -6 in our clonal EP_4-HEK293 cell line (data not shown). In addition, it has been shown that the phosphorylation of an EP_3-EP_4 chimeric receptor induced by a selective EP_3 agonist was increased in the presence of overexpressed GRK2, -3, and -5 [32].

Deletions of i3 and the C-terminal tail of EP_4 confirmed that the major determinants for EP_4 desensitization were located in the C-terminal tail. Ligand binding affinities were comparable to those of wild-type EP_4, suggesting that i3 and the C-terminal tail did not contain important determinants for PGE_2 binding or high-affinity receptor coupling. Functional assays revealed that the adenylyl cyclase response was altered by deletion of i3 (a 9-fold increase in agonist EC_{50}) and the C-terminal tail (decrease in the maximal response). These findings suggested that the coupling efficiency of EP_4 was reduced slightly by the deletions introduced in these mutants. Previous studies have highlighted the importance of conserved Glu/Arg residues at the amino terminus of i2, the NH_2 and COOH-terminal portions of i3, and the proximal portion of the C-terminal tail in coupling [39]. These regions have been left intact in the EP_4 deletion mutants. However, x-ray crystallography with bovine rhodopsin [40] and biophysical studies of the β_2-AR [41,42] have suggested that both i3 and the proximal terminus of the C-terminal tail form α-helices. It is possible that the deletions introduced in EP_4 may have affected the secondary structure of i3 and/or the C-terminal tail, thereby slightly attenuated the coupling of EP_4 with $G\alpha_s$. However, robust functional responses were achieved with the EP_4 mutants, and we were confident that they would provide a suitable model system to study the regions of EP_4 involved in desensitization.

The deletion of i3 in EP_4 did not affect its ability to desensitize, sequester, or be phosphorylated. These results are in agreement with the data showing that PKA activation did not desensitize EP_4 because deletion of the i3 loop removed the two PKA consensus phosphorylation sequences without affecting EP_4 desensitization. Truncation of the C-terminal tail at amino acid 355 significantly attenuated all the aspects of agonist-induced EP_4 desensitization, including functional activity, sequestration, and phosphorylation. Taken together, these data strongly suggest that the major determinants for agonist-induced EP_4 desensitization, sequestration, and phosphorylation are located in the C-terminal tail of the receptor.

Previous studies on EP_4 desensitization in CHO cells have focused on the waning of adenylyl cyclase activity over time. Deletion of the C-terminal tail impaired desensitization of the adenylyl cyclase activity [43], and serine residues between amino acids 370 and 382 were shown to be responsible for governing this activity [44]. In addition, other studies using EP_3-EP_4 receptor chimeras implicated the EP_4 C-terminal tail in governing the desensitization of the receptor hybrid [32]. Our studies clearly demonstrated that EP_4 desensitization is linked to both EP_4 sequestration and phosphorylation and that the C-terminal region contains the determinants responsible for all of these events.

In summary, we have described, for the first time, the agonist-mediated phosphorylation and internalization of the prostaglandin E_2 EP_4 receptor. Recent studies have highlighted the biological importance of EP_4, particularly its role in the closure of the ductus arteriosis and possibly as the mediator of PGE_2-stimulated osteogenesis, suggesting potential targets for therapeutic intervention. Promotion of bone formation would require agonist activation of EP_4. Desensitization leading to tachyphylaxis could limit the therapeutic utility of an EP_4 agonist. Therefore, we have taken the first steps in elucidating the mechanisms involved in the agonist-mediated desensitization of EP_4, thereby providing insight into its regulation.

Acknowledgments

The authors would like to thank Dr. Michel Bouvier for instructive comments and Dr. Gary O'Neill for critical reading of this manuscript.

References

[1] Coleman RA, Eglen RM, Jones RL, Narumiya S, Shimizu T, Smith WL, Dahlen SE, Drazen JM, Gardiner PJ, Jackson WT, Jones TR, Krell RD, Nicosia S. Prostanoid and leukotriene receptors: a progress report from the IUPHAR working parties on classification and nomenclature. Adv Prostaglandin Thromboxane Leukot Res 1995;23: 283–5.

[2] Katsuyama M, Nishigaki N, Sugimoto Y, Morimoto K, Negishi M, Narumiya S, Ichikawa A. The mouse prostaglandin E receptor EP_2 subtype: cloning, expression, and northern blot analysis. FEBS Lett 1995;372:151–6.

[3] Bastien L, Sawyer N, Grygorczyk R, Metters KM, Adam M. Cloning, functional expression, and characterization of the human prostaglandin E_2 receptor EP_2 subtype. J Biol Chem 1994;269:11873–7.

[4] An S, Yang J, Xia M, Goetzl EJ. Cloning and expression of the EP2 subtype of human receptors for prostaglandin E2. Biochem Biophys Res Commun 1993;197:263–70.

[5] Honda A, Sugimoto Y, Namba T, Watabe A, Irie A, Negishi M, Narumiya S, Ichikawa A. Cloning and expression of a cDNA for mouse prostaglandin E receptor EP_2 subtype. J Biol Chem 1993;268:7759–62.
[6] Breyer RM, Davis LS, Nian C, Redha R, Stillman B, Jacobson HR, Breyer MD. Differential localization of prostaglandin E receptor subtypes in human kidney. Am J Physiol 1996;270:F485–93.
[7] Nguyen M, Camenisch T, Snouwaert JN, Hicks E, Coffman TM, Anderson PAW, Malouf NN, Koller BH. The prostaglandin receptor EP_4 triggers remodelling of the cardiovascular system at birth. Nature 1997;390:78–81.
[8] Fedyk ER, Phipps RP. Prostaglandin E_2 receptors of the EP_2, and EP_4 subtypes regulate activation, and differentiation of mouse B lymphocytes to IgE-secreting cells. Proc Natl Acad Sci USA 1996;93:10978–83.
[9] Ono K, Akatsu T, Murakami T, Nishikawa M, Yamamoto M, Kugai N, Motoyoshi K, Nagata N. Important role of EP_4, a subtype of prostaglandin (PG) E receptor, in osteoclast-like cell formation from mouse bone marrow cells induced by PGE_2. J Endocrinol 1998;158:R1–5.
[10] Weinreb M, Grosskopf A, Shir N. The anabolic effect of PGE_2 in rat bone marrow cultures is mediated via the EP_4 receptor subtype. Am J Physiol 1999;276:E376–83.
[11] Machwate M, Harada S, Leu CT, Seedor G, Labelle M, Gallant M, Hutchins S, Lachance N, Sawyer N, Slipetz D, Metters KM, Rodan SB, Young R, Rodan GA. Prostaglandin receptor EP_4 mediates the bone anabolic effects of PGE_2. Mol Pharmacol 2001;60:36–41.
[12] Funk CD. Molecular biology in the eicosanoid field. Prog Nucleic Acid Res Mol Biol 1993;45:67–98.
[13] Smith WL. Prostanoid biosynthesis and mechanisms of action. Am J Physiol 1992;263:F181–91.
[14] Jakobsson PJ, Thoren S, Morgenstern R, Samvelsson B. Identification of human prostaglandin E synthase: a microsomal, glutathione-dependent, inducible enzyme, constituting a potential novel drug target. Proc Natl Acad Sci USA 1999;96:7220–5.
[15] Kanai N, Lu R, Satriano JA, Bao Y, Wolkoff AW, Schuster VL. Identification and characterization of a prostaglandin transporter. Science 1995;268:866–9.
[16] Nishigaki N, Negishi M, Ichikawa A. Two G_s-coupled prostaglandin E receptor subtypes, EP2, and EP4, differ in desensitization, and sensitivity to the metabolic inactivation of the agonist, Mol Pharmacol 1996;50:1031–7.
[17] Bunemann M, Hosey MM. G-protein coupled receptor kinases as modulators of G-protein signalling. J Physiol (Lond) 1999;517:5–23.
[18] Pitcher JA, Freedman NJ, Lefkowitz RJ. G protein-coupled receptor kinases. Annu Rev Biochem 1998;67:653–92.
[19] Lefkowitz RJ. G protein-coupled receptors. III. New roles for receptor kinases and β-arrestins in receptor signaling and desensitization. J Biol Chem 1998;273:18677–80.
[20] Krupnick JG, Benovic JL. The role of receptor kinases and arrestins in G protein-coupled receptor regulation. Annu Rev Pharmacol Toxicol 1998;38:289–319.
[21] Goodman OB Jr, Krupnick JG, Santini F, Gurevich VV, Penn RB, Gagnon AW, Keen JH, Benovic JL. β-Arrestin acts as a clathrin adaptor in endocytosis of the β_2-adrenergic receptor. Nature 1996;383:447–50.
[22] Smith DB, Johnson KS. Single-step purification of polypeptides expressed in *Escherichia coli* as fusions with glutathione *S*-transferase. Gene 1988;67:31–40.
[23] Abramovitz M, Adam M, Boie Y, Carrière M-C, Denis D, Godbout C, Lamontagne S, Rochette C, Sawyer N, Tremblay NM, Belley M, Gallant M, Dufresne C, Gareau Y, Ruel R, Juteau H, Labelle M, Ouimet N, Metters KM. The utilization of recombinant prostanoid receptors to determine the affinities and selectivities of prostaglandins and related analogs. Biochim Biophys Acta 2000;1483:285–93.
[24] Salomon Y, Londos C, Rodbell M. A highly sensitive adenylate cyclase assay. Anal Biochem 1974;58:541–8.
[25] Sambrook J, Fritsch EF, Maniatis T. Molecular cloning: a laboratory manual. 2nd Ed. Cold Spring Harbor, NY: Cold Spring Harbor Laboratory, 1989.
[26] Whitehead TP, Kricka LJ, Carler TJ, Thorpe GH. Analytical luminescence: its potential in the clinical laboratory. Clin Chem 1979;25:1531–46.
[27] Premont RT, Inglese J, Lefkowitz RJ. Protein kinases that phosphorylate activated G protein-coupled receptors. FASEB J 1995;9:175–82.
[28] Chuang TT, Iacovelli L, Sallese M, De Blasi A. G protein coupled receptors: heterologous regulation of homologous desensitization, and its implications. Trends Pharmacol Sci 1996;17:416–21.
[29] Zhang J, Barak LS, Anborgh PH, Laporte SA, Caron MG, Ferguson SSG. Cellular trafficking of G protein-coupled receptor/β-arrestin endocytic complexes. J Biol Chem 1999;274:10999–1006.
[30] Ferguson SSG, Downey WE III, Colapietro A-M, Barak LS, Ménard L, Caron MG. Role of β-arrestin in mediating agonist-promoted G protein-coupled receptor internalization. Science 1996;271:363–6.
[31] Laporte SA, Oakley RH, Zhang J, Holt JA, Ferguson SSG, Caron MG, Barak LS. The β_2-adrenergic receptor/βarrestin complex recruits the clathrin adaptor AP-2 during endocytosis. Proc Natl Acad Sci USA 1999;96:3712–7.
[32] Neuschäfer-Rube F, Oppermann M, Möller U, Böer U, Püschel GP. Agonist-induced phosphorylation by G protein-coupled receptor kinases of the EP4 receptor carboxyl-terminal domain in an EP3/EP4 prostaglandin E_2 receptor hybrid. Mol Pharmacol 1999;56:419–28.
[33] Onorato JJ, Palczewski K, Regan JW, Caron MG, Lefkowitz RJ, Benovic JL. Role of acidic amino acids in peptide substrates of the β-adrenergic receptor kinase and rhodopsin kinase. Biochemistry 1991;30:5118–25.
[34] Eason MG, Moreira SP, Liggett SB. Four consecutive serines in the third intracellular loop are the sites for β-adrenergic receptor kinase-mediated phosphorylation and desensitization of the α_{2A}-adrenergic receptor. J Biol Chem 1995;270:4681–8.
[35] Prossnitz ER, Kim CM, Benovic JL, Ye RD. Phosphorylation of the *N*-formyl peptide receptor carboxyl terminus by the G protein-coupled receptor kinase GRK2. J Biol Chem 1995;270:1130–7.
[36] Giannini E, Brouchon L, Boulay F. Identification of the major phosphorylation sites in human C5a anaphylatoxin receptor *in vivo*. J Biol Chem 1995;270:19166–72.
[37] Diviani D, Lattion A-L, Cotecchia S. Characterization of the phosphorylation sites involved in G protein-coupled receptor kinase- and protein kinase C-mediated desensitization of the α_{1B}-adrenergic receptor. J Biol Chem 1997;272:28712–9.
[38] Seibold A, January BG, Friedman J, Hipkin RW, Clark RB. Desensitization of β_2-adrenergic receptors with mutations of the proposed G protein-coupled receptor kinase phosphorylation sites. J Biol Chem 1998;273:7637–42.
[39] Wess J. G-protein-coupled receptors: molecular mechanisms involved in receptor activation, and selectivity of G-protein recognition. FASEB J 1997;11:346–54.
[40] Palczewski K, Kumasaka T, Hori T, Behnke CA, Motoshima H, Fox BA, Le Trong I, Teller DC, Okada T, Stenkamp RE, Yamamoto M, Miyano M. Crystal structure of rhodopsin: a G protein-coupled receptor. Science 2000;289:739–45.
[41] Jung H, Windhaber R, Palm D, Schnackerz KD. NMR, and circular dichroism studies of synthetic peptides derived from the third intracellular loop of the β-adrenoceptor. FEBS Lett 1995;358:133–6.
[42] Jung H, Windhaber R, Palm D, Schnackerz KD. Conformation of a β-adrenoceptor-derived signal transducing peptide as inferred by circular dichroism and ^{1}H NMR spectroscopy. Biochemistry 1996;35:6399–405.
[43] Bastepe M, Ashby B. The long cytoplasmic carboxyl terminus of the prostaglandin E_2 receptor EP_4 subtype is essential for agonist-induced desensitization. Mol Pharmacol 1997;51:343–9.
[44] Bastepe M, Ashby B. Identification of a region of the C-terminal domain involved in short-term desensitization of the prostaglandin EP4 receptor. Br J Pharmacol 1999;126:365–71.